METAHEURISTIC OPTIMIZATION OF A MODIFIED TUNED INERTER DAMPER FOR SEISMICALLY LOADED STRUCTURES

L. Lara(1), J. Rendón(2), Y. Farbiarz(3), D. Caicedo(4), M. Ramírez(5)

(1) Associate Professor, Universidad Nacional de Colombia, Facultad de Minas, Sede Medellín, Departamento de Ingeniería Civil, Medellín, Colombia, lualarava@unal.edu.co
(2) Master Student, Universidad Nacional de Colombia, Facultad de Minas, Sede Medellín, Departamento de Ingeniería Civil, Medellín, Colombia, jfrendong@unal.edu.co
(3) Titular Professor, Universidad Nacional de Colombia, Facultad de Minas, Sede Medellín, Departamento de Ingeniería Civil, Medellín, Colombia, jfarbiar@unal.edu.co
(4) Civil Engineer, Universidad Nacional de Colombia, Facultad de Minas, Sede Medellín, Departamento de Ingeniería Civil, Medellín, Colombia, dcaicedod@unal.edu.co
(5) Undergrade Student, Universidad Nacional de Colombia, Facultad de Minas, Sede Medellín, Departamento de Ingeniería Civil, Medellín, Colombia, maramirezac@unal.edu.co

Abstract

The control of structural response under seismic loads is a rapidly growing field in most of the countries seismically active, as an alternative to the conventional design methodologies that are based on a ductile response. The design of buildings including structural control may result in smaller element dimensions and larger column spans, which, in turn, may reduce construction costs and increase space usage. This paper presents a numerical investigation on the optimization procedure for the design parameters of a Tuned Inerter Damper (TID) device. The classical location of the TID is changed from the base of the building to the last two levels to control the vibrations induced by seismic loads. A metaheuristic technique based on Differential Evolution (DE) is used to define the optimal design parameters of a TID device. The frequency (f) and damping (ζd) ratios that minimize the structure response are obtained through an objective function that aims to minimize the horizontal peak displacements and the root mean square (RMS) of displacements. To verify the methodology, a 11-story case-study building equipped with an optimized TID device is analyzed. The performance of the TID located in the last two levels of a structure was compared with the performance of the TID located on the first level. A sensitivity analysis was conducted for the selection of the seismic records which are expected to have a greater impact on the structure response. The results show that the proposed methodology is effective in finding the optimal configuration for the TID design parameters that reduce the structural response.

Keywords: Tuned inerter damper; Differential evolution; Optimization procedure; Structural control; Sensitivity analysis.

1. Introduction

Passive controllers are possibly the best known and widely accepted systems for the mitigation of seismic induced vibrations. Among them, the Tuned Inerter Damper (TID) offers an attractive alternative to conventional Tuned Mass Dampers (TMDs) since a high level of vibration control can be achieved with relatively small amounts of added mass to the buildings [1]. The main component of the TID is the inerter device, originally proposed by Smith [2] in the early 2000s as a two-terminal mechanical device, with the property that the equal and opposite forces at its terminals are proportional to the relative acceleration between them. Thus, the TID takes advantage of the apparent mass amplification effect induced by the inerter.

The inerter can provide significant improvements in the performance of various mechanical systems, such as vehicle suspensions, train suspensions, building and bridge vibration control systems [2]. Wang et al. [3, 4] and Chen et al. [5] studied different TID schemes for building vibration control and performed some experimental tests using ball-screw-based inerters as well. Lazar et al. [1, 6, 7, 8] and Wen et al. [9]

evaluated the TID performance on MDOF structures, using the device as a brace between two different floors, and compared its performance with the classical TMDs. Similarly, Zhang et al. [10] studied the response of MDOF structures equipped with multiple TIDs. Pan & Zhang [11] implemented an optimization method that considers the stochastic vibration response mitigation ratio as a design index to solve the tunning problem. On the other hand, Shen et al. [12] used the fixed-point-theory to determine simple design formulas for the TID in a single-degree-of-freedom system. Radu et al. [13] proposed a fully probabilistic framework for the performance-based seismic design of TIDs. Caicedo [14] compared the TID and TMDI devices performance for buildings vibration control using a metaheuristic optimization procedure for the device parameters selection.

This paper presents a numerical study for the optimal parameter selection of a modified TID scheme. In this arrangement, the location of the device is changed from the ground-story to the last two story-levels of the structural system. The optimization process is carried out using Differential Evolution (DE) based metaheuristic, in which the optimal frequency (f) and damping (ζ_d) ratios are found for minimizing the horizontal peak displacements and the root mean square (RMS) of displacements. The proposed methodology is applied to a case-study building located in Medellín city (Colombia) considering the seismic records derived from a sensitivity analysis. The performance of the TID located in the last two levels of a structure is compared with the performance of a TID located on the first level. The results show that the proposed methodology is effective in finding the optimal set of design parameters that reduce considerably the structural response.

2. Mathematical model of a MDOF structure equipped with a TID

The inerter is a mechanical device that links two nodes (terminals), free to move independently, where the equal and opposite forces at its terminals are proportional to the relative acceleration between them [2], as is shown in Fig.1.

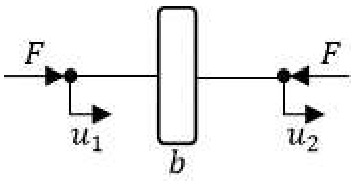

$$F = b(\ddot{u}_2 - \ddot{u}_1)$$

Fig. 1 – Inerter idealization

Where and are the acceleration applied in the terminals and b denotes the inertance value.

As mentioned above, TID are passive structural control systems whose main advantage is that it is possible to achieve a high level of vibration control with a relatively small device mass in comparison with other systems such as TMDs [1]. Fig.2 shows the TID layout.

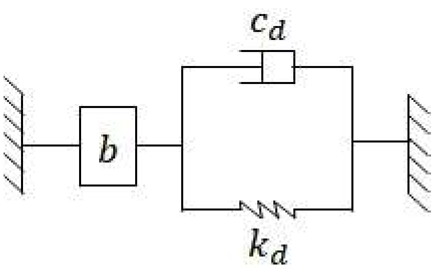

Fig. 2 – TID Scheme

Fig.3 shows a 2D Frame modeled as a shear building, with n-DOF related to the horizontal displacement of each story level, equipped with a TID device as a brace between the last two levels, where m_i, k_i and c_i are the mass, lateral stiffness and damping of the i^{th} floor ($i=1, 2, ..., n$) and k_d and c_d are stiffness and damping that defined the TID behavior. This last two variables can be expressed as follows:

$$k_d = \omega_s^2 f^2 b \tag{1}$$

$$c_d = 2 f \xi_d \omega_s b \tag{2}$$

where w_s, f and ξ_d are the fundamental circular frequency of the structural system, the frequency and damping ratios between the structure and the TID. In this way, the tunning procedure focus on finding the optimal frequency and damping ratios that minimize the structure response.

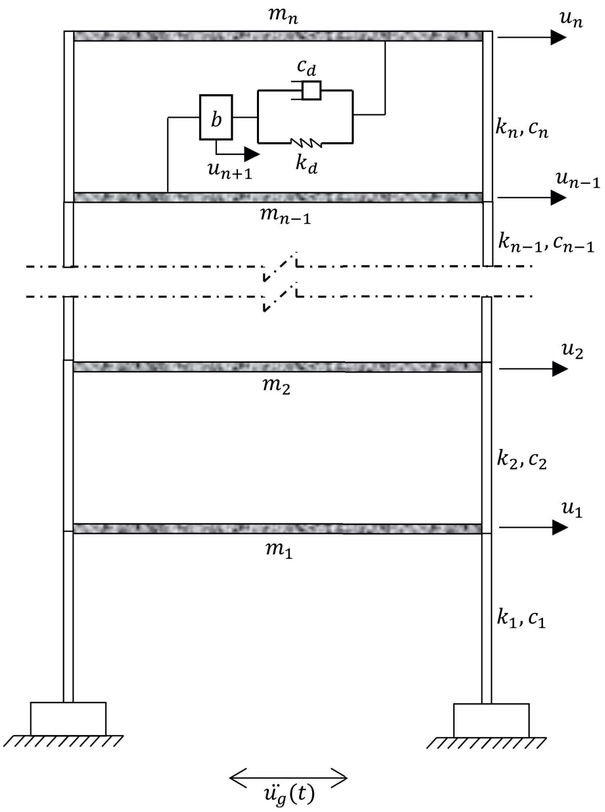

Fig. 3 – 2D frame equipped with a TID in the last two levels

The following dynamic equilibrium equations describe the behavior of the structural system defined in Fig.3, including the additional degree of freedom ($n+1$) given by the possibility of horizontal movement of the TID.

$$m_1\ddot{u}_1 + (c_1 + c_2)\dot{u}_1 - c_2\dot{u}_2 + (k_1 + k_2)u_1 - k_2u_2 = -m_1\ddot{u}_g(t) \tag{3}$$

$$m_2\ddot{u}_2 - c_2\dot{u}_1 + (c_2 + c_3)\dot{u}_2 - c_3\dot{u}_3 - k_2u_1 + (k_2 + k_3)u_2 - k_3u_3 = -m_2\ddot{u}_g(t) \tag{4}$$

$$\begin{aligned} m_{n-1}\ddot{u}_{n-1} - c_{n-1}\dot{u}_{n-2} + (c_{n-1} + c_n + c_d)\dot{u}_{n-1} - c_n\dot{u}_n - c_d\dot{u}_{n+1} - k_{n-1}u_{n-2} + (k_{n-1} + k_n + k_d)u_{n-1} \\ - k_nu_n - k_du_{n+1} = -m_{n-1}\ddot{u}_g(t) \end{aligned} \tag{5}$$

$$m_n\ddot{u}_n - c_n\dot{u}_{n-1} + (c_n + c_d)\dot{u}_n - c_n\dot{u}_n - c_d\dot{u}_{n+1} - k_nu_{n-1} + (k_n + k_d)u_n - k_du_d = -m_n\ddot{u}_g(t) \tag{6}$$

$$b\ddot{u}_{n+1} - c_d\dot{u}_{n-1} - c_d\dot{u}_n + c_d\dot{u}_{n+1} - k_du_{n-1} - k_du_n + k_du_{n+1} = -m_b\ddot{u}_g(t) \tag{7}$$

It is worth noting that in the Eq. (7), the inertial load produced by the ground acceleration depends of the TID's physical mass (m_b), which can be expressed as follows:

$$b = 200m_b \rightarrow m_b = \frac{1}{200}b \tag{8}$$

The constant *1/200* denotes the ratio between the TID's physical mass and the inertance. This ratio is assumed according to Papageorgiou and Smith [15] and Papageorgiou et al. [16].

Now, by reorganizing Eq. (3) - (7) the system may be written in matrix form as:

$$\boldsymbol{M}\ddot{\boldsymbol{U}}(t) + \boldsymbol{C}\dot{\boldsymbol{U}}(t) + \boldsymbol{K}\boldsymbol{U}(t) = -\boldsymbol{M}\{\boldsymbol{\delta}\}\ddot{\boldsymbol{u}}_g(t) \tag{9}$$

$$\boldsymbol{M} = \begin{bmatrix} m_1 & 0 & \cdots & 0 & 0 & 0 \\ 0 & m_2 & \cdots & 0 & 0 & 0 \\ \vdots & \vdots & \ddots & \vdots & \vdots & \vdots \\ 0 & 0 & \cdots & m_{n-1} & 0 & 0 \\ 0 & 0 & \cdots & 0 & m_n & 0 \\ 0 & 0 & \cdots & 0 & 0 & b \end{bmatrix} \tag{10}$$

$$\boldsymbol{C} = \begin{bmatrix} c_1 + c_2 & -c_2 & \cdots & 0 & 0 & 0 \\ -c_2 & c_2 + c_3 & \cdots & 0 & 0 & 0 \\ \vdots & \vdots & \ddots & \vdots & \vdots & \vdots \\ 0 & 0 & \cdots & c_{n-1} + c_n + c_d & -c_n & -c_d \\ 0 & 0 & \cdots & -c_n & c_n + c_d & -c_d \\ 0 & 0 & \cdots & -c_d & -c_d & c_d \end{bmatrix} \tag{11}$$

$$\boldsymbol{K} = \begin{bmatrix} k_1 + k_2 & -k_2 & \cdots & 0 & 0 & 0 \\ -k_2 & k_2 + k_3 & \cdots & 0 & 0 & 0 \\ \vdots & \vdots & \ddots & \vdots & \vdots & \vdots \\ 0 & 0 & \cdots & k_{n-1} + k_n + k_d & -k_n & -k_d \\ 0 & 0 & \cdots & -k_n & k_n + k_d & -k_d \\ 0 & 0 & \cdots & -k_d & -k_d & k_d \end{bmatrix} \tag{12}$$

$$\boldsymbol{U} = \{u_1 \quad u_2 \quad \cdots \quad u_{n-1} \quad u_n \quad u_{n+1}\}^T \tag{13}$$

$$\boldsymbol{\delta} = \{1 \quad 1 \quad \cdots \quad 1 \quad 1 \quad 1/200\}^T \tag{14}$$

where *M*, *C* and *K* are the mass, stiffness and damping matrices, and *U* is defined as the structure displacement response.

3. Differential Evolution Optimization, DE

DE is a parallel direct search method introduced by Storn and Price in 1996 [17] based on a population stochastic-approach for solving global optimization problems [18]. DE can be summarized in four stages and a final decision, as shown in Fig.4.

Stage I – Initialization: DE utilizes NP parameter vectors as population for each generation; the initial population is chosen randomly with a uniform probability distribution according to the range defined for each parameter.

Stage II – Mutation: For each generation, new parameter vectors are generated by adding the weighted difference vector between two population members into a third one.

Stage III- Recombination: To aid to the diversity of mutation vectors, these vectors are modified by combining them with a predetermined population member according to the probability of crossover.

Stage IV – Selection: If the resulting vectors yield a lower value in the cost function than the predetermined population member used in the recombination, the newly generated vector replaces the vector with which it was compared.

Convergence criterion: At the end of stage IV, if the convergence defined for the objective function is achieved or the maximum number of iterations is reached, the vector provides the optimal solution, otherwise, the optimization returns to stage II.

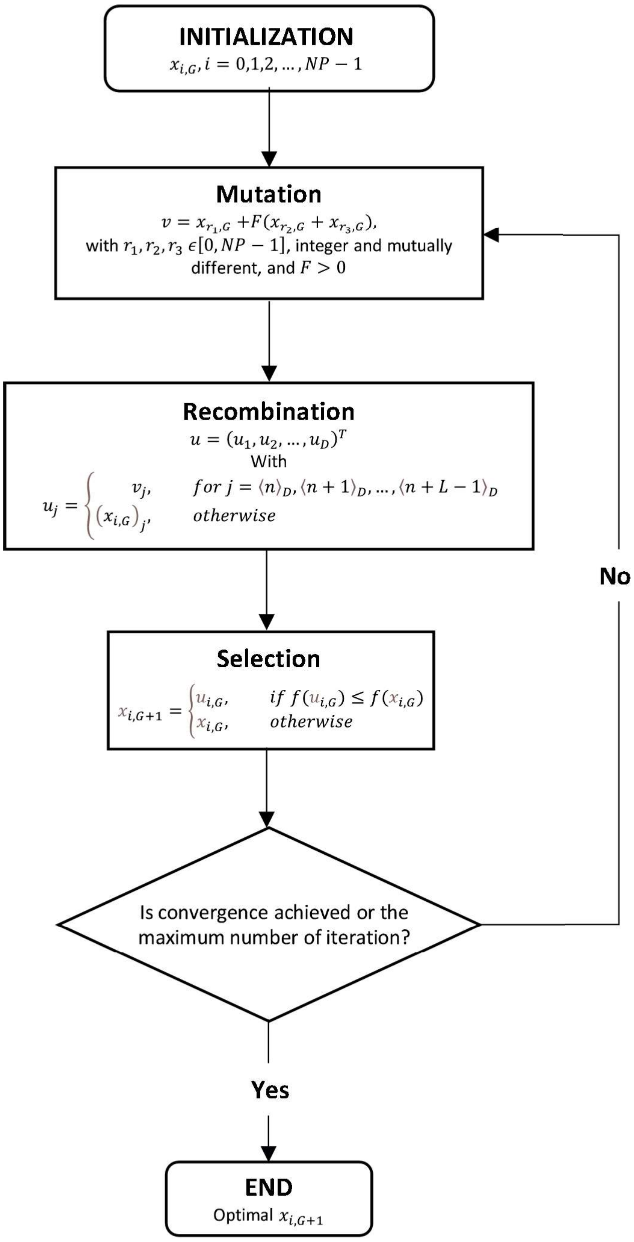

Fig. 4 – DE procedure description

The objective function defined for the TID optimization aims to minimize the horizontal peak displacements and the root mean square (RMS) of the displacements. These objective functions evaluate the ratio between the controlled response via TID and the uncontrolled response of the system focused at the n^{th} degree of freedom and are described as follow:

$$F_{obj1} = \frac{\max(n^{th}\ DOF\ displacement\ controlled\ response)}{\max(n^{th}\ DOF\ displacement\ uncontrolled\ response)} \tag{15}$$

$$F_{obj2} = \frac{\text{RMS of the } n^{th}\ DOF\ controlled\ response}{\text{RMS of the } n^{th}\ DOF\ uncontrolled\ response} \tag{16}$$

4. Case-Study

The Beneficencia de Antioquia building, which houses the public lottery agency of Medellin city, was selected as case study in this investigation. The building has 11 levels, each with 2,72 m of height, for a total of 31,14 m above the ground level. The building structure is comprised of a combination of two different lateral-force-resisting systems, reinforced concrete moment-resisting frames in the direction parallel to the front facade of the building, and reinforced concrete moment-resisting frames and structural walls dual system in the perpendicular direction. Fig.5 shows the case-study building and a 3D model performed in MIDAS GEN, from which a frame was taken in the direction of the main facade that was simplified and modeled as a 2D-frame to assess the behavior of the TID as shown in Fig.6.

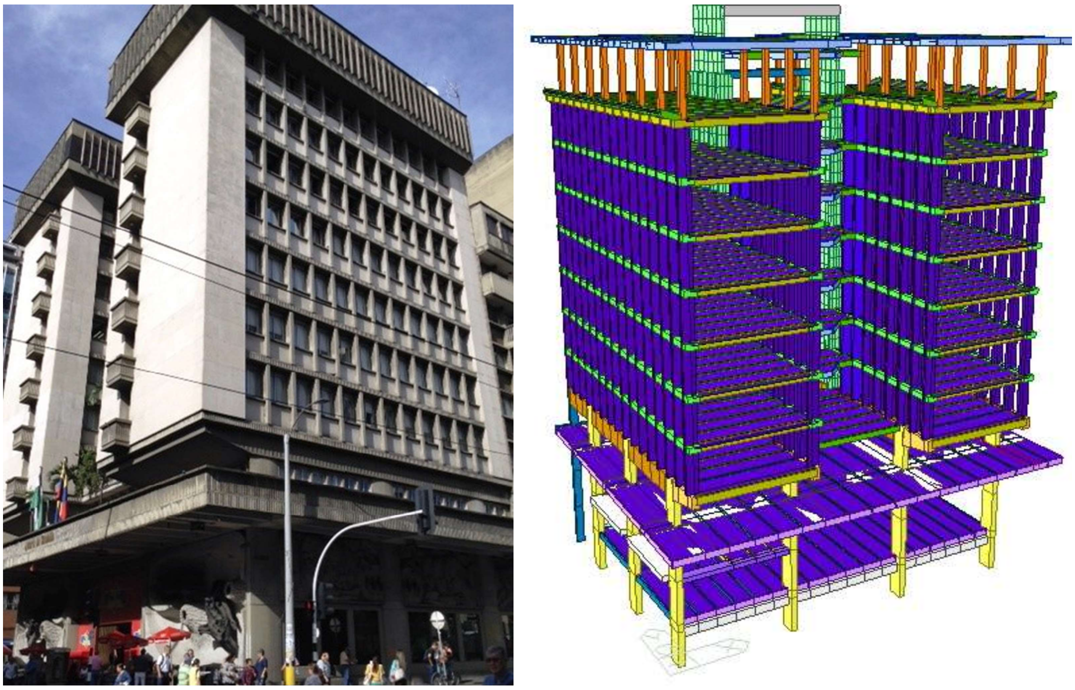

Fig. 5 – General view and 3D model of the building Beneficencia de Antioquia

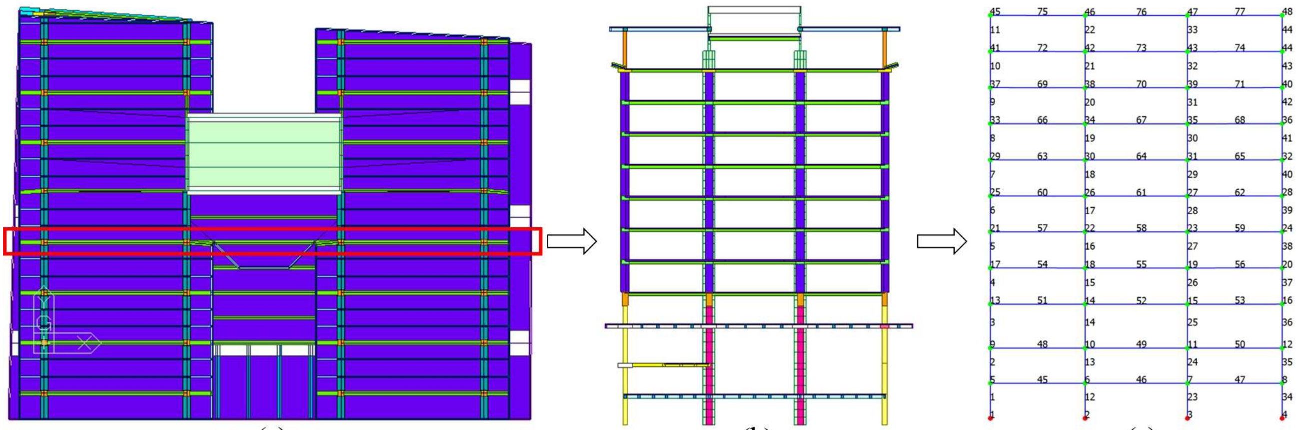

(a) (b) (c)

Fig. 6 – Structure details. (a) Typical floor plan of the building. (b) Plane frame chosen for modeling. (c) Modeled simplified frame

5. Seismic Loads

The seismic loads are represented by a set of four accelerograms taken from the Pacific Earthquake Engineering Research (PEER) Centre database [19]. These records were selected based on their predominant period by means of a sensitivity analysis to verify the structure excitation. Table 1 shows a summary of the sensitivity analysis.

Table 1 – Sensitivity analysis summary

		T [s]	PGA [g]	U_{max} [mm]
1	Northridge	0.31	0.600	730.1
2	Tokachi	1.20	0.186	531.6
3	Kobe	1.21	0.670	1 074
4	San Fernando	0.21	1.170	601.7

It is worth noting that seismic records like Tokachi with a low ground acceleration and a period of 1.2 s, which can be considered as a long period earthquake, are likely to have a considerable impact on the structure's response.

6. Results

Table 2 and 3 report the optimal values for both cost functions considered in the optimization process. It is clear that the reductions in the dynamic response, measured by the cost function value, are significantly better when the device is located in the last two levels of the structure than when it is located at the base.

Table 2 – Optimal Cost Function values

		TID on the last two levels		TID at the base	
		F_{obj1}	F_{obj2}	F_{obj1}	F_{obj2}
1	Northridge	0.80	0.51	1.00	0.98
2	Tokachi	0.53	0.31	0.99	0.99
3	Kobe	0.70	0.49	1.00	0.99
4	San Fernando	0.75	0.46	1.00	0.99

Table 3 – Optimal design parameter for the TID located on the last two levels of the structure

		F_{obj1}		F_{obj2}	
		f	ζ_d	f	ζ_d
1	Northridge	1.00	4.08E-04	1.01	1.45E-01
2	Tokachi	1.09	7.16E-03	1.02	7.17E-02
3	kobe	1.27	1.94E-02	0.97	1.16E-01
4	San Fernando	1.10	2.18E-04	0.98	7.09E-02

Table 4 shows the maximum displacement and RMS of the 11th story values for both objective function and for each seismic record.

Table 4 – Maximum displacement of the 11th story and RMS of 11th story

			F_{obj1}		F_{obj2}	
	Seismic Record	**Uncontrolled Response**	**TID at the last two levels**	**% Reduction**	**TID at the last two levels**	**% Reduction**
11^{th} u_{Max} [mm]	Northridge	787.1	657.5	20.39%	692.1	12.07%
	Tokachi	627.4	329.6	47.46%	365.5	41.74%
	Kobe	1228.1	858.5	30.09%	1041	15.23%
	San Fernando	866.6	651.7	24.79%	654.7	24.45%
11^{th} RMS [mm]	Northridge	236.8	252.5	-6.63%	121.7	48.61%
	Tokachi	336.8	138.9	58.76%	103.4	69.30%
	kobe	618.4	473.5	23.43%	304.8	50.71%
	San Fernando	367.5	219.3	40.33%	167.5	54.42%

Fig.7 - 8 show the displacement of the 11^{th} story and the RMS of the displacements of all horizontal degrees of freedom, for each seismic record, in order to compare the efficiency of the TID device located in the last two levels of the structure against the TID at the base, in reducing the top-story (11^{th} story) dynamic displacement.

On average, the reductions of the structure response attained with the TID installed at the base are 0,45% for the first objective function, F_{obj1}, and 1,05% for the second objective function F_{obj2}; while for the TID installed on the last two levels of the structure the reductions are much greater, 30,68% for F_{obj1} and 55,84% for F_{obj2}. The maximum reduction is around 69% for F_{obj2} under Tokachi's record.

The results show that the optimization procedure using the cost function F_{obj1} allows significant reductions, which oscillates between 20% to 47% of the maximum displacements. In these circumstances, there are cases where the device increases the response of the structure for times different from that of the maximum displacement as can be seen in Fig.7(a).

On the other hand, cost function F_{obj2} not only enables important reductions, which oscillates between 49% to 69%, on the n^{th} RMS, but also provided significant reductions, which oscillates between 12% to 42% of the nth maximum displacement which is comparable with the reductions attained with cost function F_{obj1}.

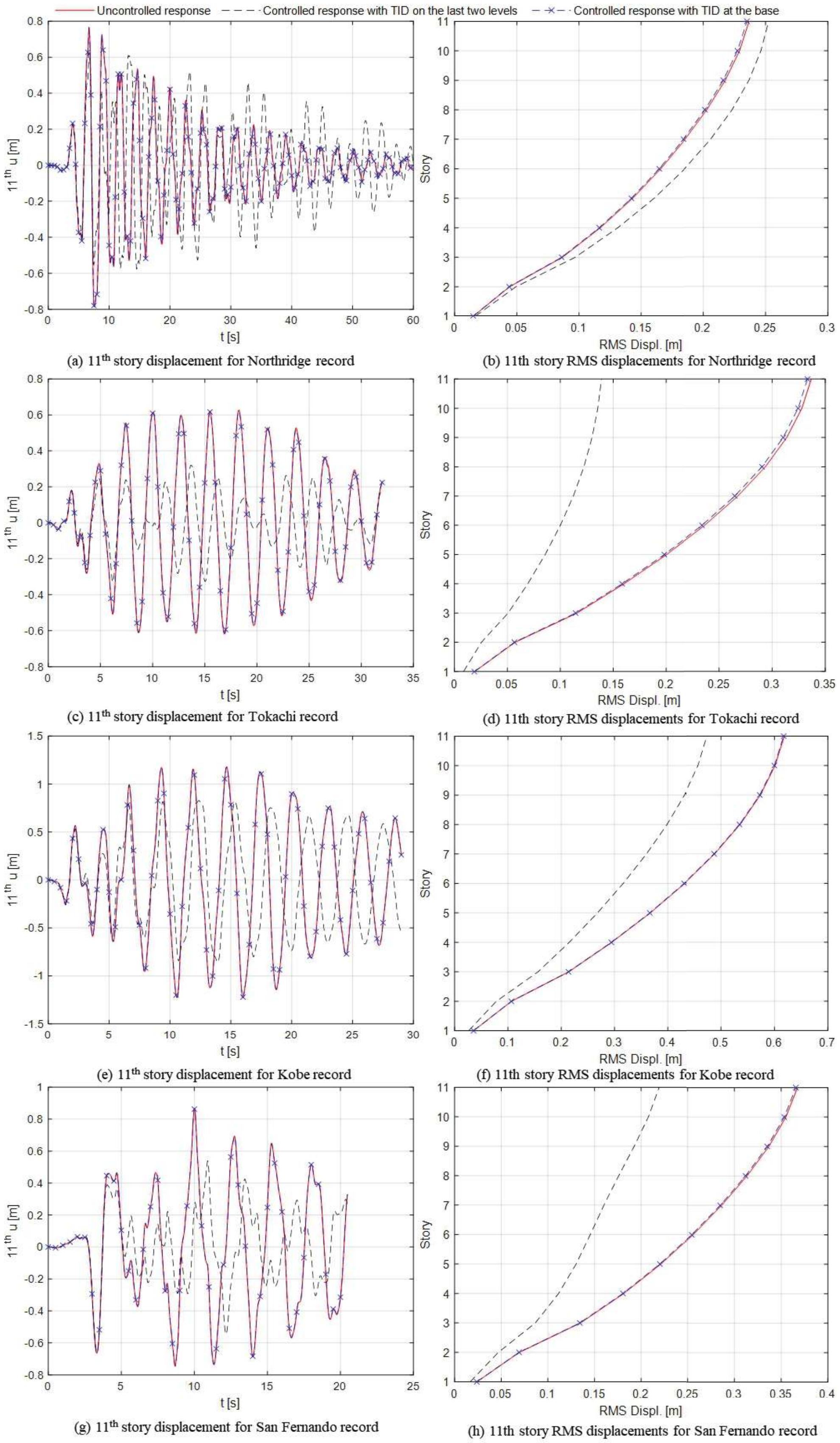

(a) 11th story displacement for Northridge record
(b) 11th story RMS displacements for Northridge record
(c) 11th story displacement for Tokachi record
(d) 11th story RMS displacements for Tokachi record
(e) 11th story displacement for Kobe record
(f) 11th story RMS displacements for Kobe record
(g) 11th story displacement for San Fernando record
(h) 11th story RMS displacements for San Fernando record

Fig. 7 – Optimal design parameters derived from F_{obj1}

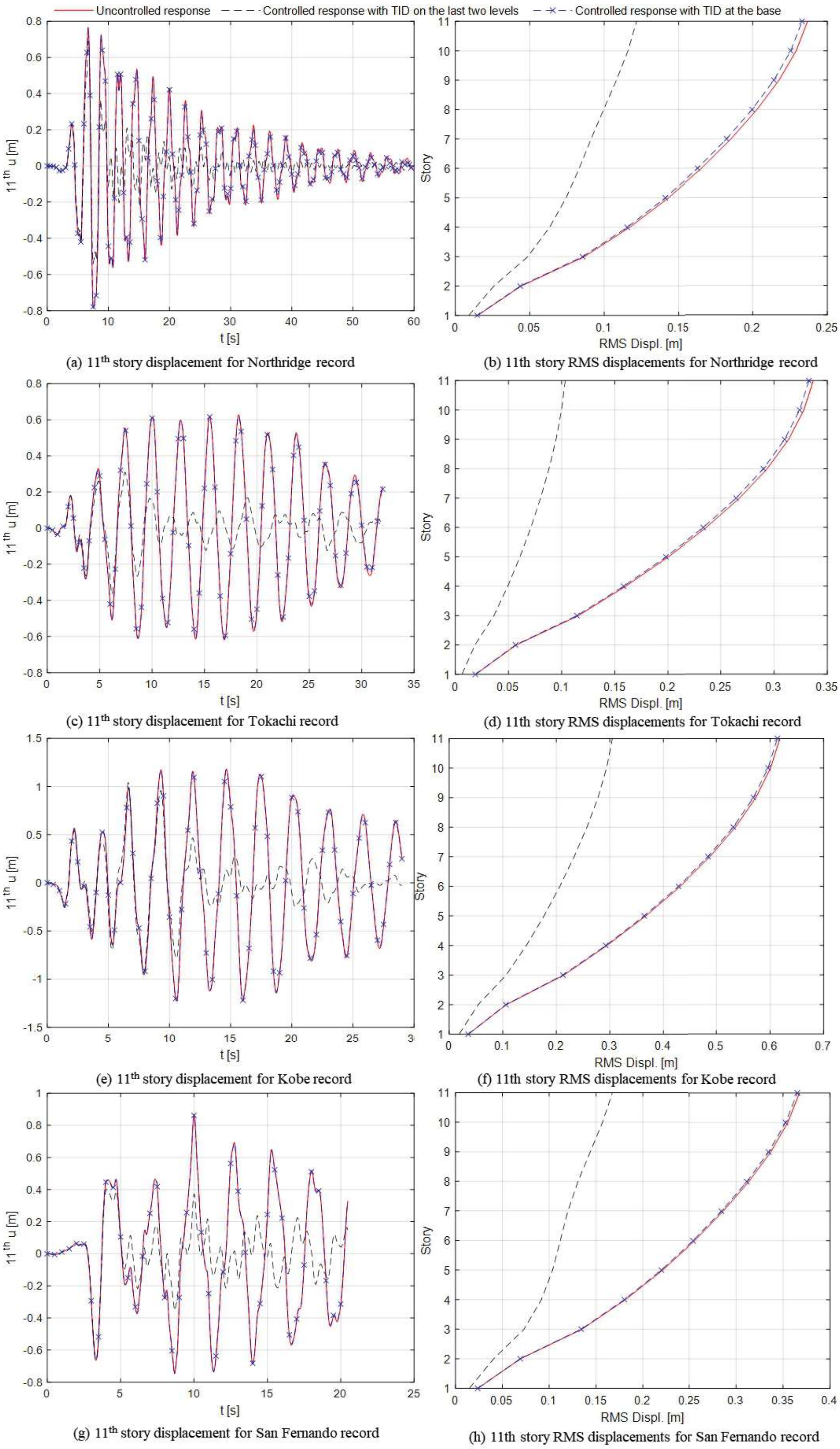

(a) 11th story displacement for Northridge record
(b) 11th story RMS displacements for Northridge record
(c) 11th story displacement for Tokachi record
(d) 11th story RMS displacements for Tokachi record
(e) 11th story displacement for Kobe record
(f) 11th story RMS displacements for Kobe record
(g) 11th story displacement for San Fernando record
(h) 11th story RMS displacements for San Fernando record

Fig. 7 – Optimal design parameters derived from F_{obj2}

7. Conclusions

As mentioned above, TID located in the last two level of the structure show a better structural control than a TID located at the base.

As for the cost function F_{obj2}, which aims to minimize the nth RMS, it allows to obtain the best reductions in the response of the structure and a better control of the response over time, significantly reducing the displacements of the structure during the seismic event.

Finally, regarding the optimization procedure used, it can be concluded that it presents a relatively fast convergence and that, as many authors have mentioned, the computational cost is low.

8. Acknowledgements

The acknowledgements provide an opportunity to express appreciation to those who contributed significantly to the preparation of the paper. They may be written in free style, and must be brief.

9. Copyrights

10. References

[1] Lazar, I. F., Neild, S. A., & Wagg, D. J. (2014). Using an inerter-based device for structural vibration suppression. Earthquake Engineering & Structural Dynamics, 43(8), 1129-1147.

[2] Chen, M. Z., & Hu, Y. (2019). Inerter and Its Application in Vibration Control Systems. Springer Singapore.

[3] Wang, F. C., Chen, C. W., Liao, M. K., & Hong, M. F. (2007, December). Performance analyses of building suspension control with inerters. In 2007 46th IEEE Conference on Decision and Control (pp. 3786-3791). IEEE.

[4] Wang, F. C., Hong, M. F., & Chen, C. W. (2010). Building suspensions with inerters. Proceedings of the Institution of Mechanical Engineers, Part C: Journal of Mechanical Engineering Science, 224(8), 1605-1616.

[5] Chen, Y. C., Tu, J. Y., & Wang, F. C. (2015, July). Earthquake vibration control for buildings with inerter networks. In 2015 European Control Conference (ECC) (pp. 3137-3142). IEEE.

[6] Lazar, I. F., Wagg, D. J., & Nield, S. A. (2013). An inerter vibration isolation system for the control of seismically excited structures, Int. In Conf. Urban Earthq. Eng.

[7] Lazar, I. F., Neild, S. A., & Wagg, D. J. (2014). Inerter-based vibration suppression systems for laterally and base-excited structures. In Proceedings of EURODYN 2014 (pp. 1525-1530). Sheffield.

[8] Lazar, I. F., Neild, S. A., & Wagg, D. J. (2014). Design and performance analysis of inerter-based vibration control systems. In Dynamics of Civil Structures, Volume 4 (pp. 493-500). Springer, Cham.

[9] Wen, Y., Chen, Z., & Hua, X. (2017). Design and evaluation of tuned inerter-based dampers for the seismic control of MDOF structures. Journal of Structural Engineering, 143(4), 04016207.

[10] Zhang, S. Y., Lewis, T. D., Jiang, J. Z., & Neild, S. A. (2016). Passive vibration suppression using multiple inerter-based devices for a multi-storey building structure. In Proceedings of the 6th European Conference on Structural Control, Sheffield, United Kingdom.

[11] Pan, C., & Zhang, R. (2018). Design of structure with inerter system based on stochastic response mitigation ratio. Structural Control and Health Monitoring, 25(6), e2169.

[12] Shen, W., Niyitangamahoro, A., Feng, Z., & Zhu, H. (2019). Tuned inerter dampers for civil structures subjected to earthquake ground motions: optimum design and seismic performance. Engineering Structures, 198, 109470.

[13] Radu, A., Lazar, I. F., & Neild, S. A. (2019). Performance-based seismic design of tuned inerter dampers. Structural Control and Health Monitoring, 26(5), e2346.

[14] Caicedo Diaz, D. A. A comparative analysis on the seismic behavior of buildings using inerter-based devices: Tuned Mass Damper Inerter (TMDI) and Tuned Inerter Damper (TID).

[15] Papageorgiou, C., & Smith, M. C. (2005, December). Laboratory experimental testing of inerters. In Proceedings of the 44th IEEE Conference on Decision and Control (pp. 3351-3356). IEEE.

[16] Papageorgiou, C., Houghton, N. E., & Smith, M. C. (2009). Experimental testing and analysis of inerter devices. Journal of dynamic systems, measurement, and control, 131(1).

[17] Storn, R., & Price, K. (1997). Differential evolution–a simple and efficient heuristic for global optimization over continuous spaces. Journal of global optimization, 11(4), 341-359.

[18] Chakraborty, U. K. (Ed.). (2008). Advances in differential evolution (Vol. 143). Springer.

[19] Pacific Earthquake Engineering Research Center: Ground Motion Database. Available: http://peer.berkeley.edu/peer_ground_motion_database

